

UNCLASSIFIED

AD 404 848

DEFENSE DOCUMENTATION CENTER

FOR

SCIENTIFIC AND TECHNICAL INFORMATION

CAMERON STATION, ALEXANDRIA, VIRGINIA



UNCLASSIFIED

NOTICE: When government or other drawings, specifications or other data are used for any purpose other than in connection with a definitely related government procurement operation, the U. S. Government thereby incurs no responsibility, nor any obligation whatsoever; and the fact that the Government may have formulated, furnished, or in any way supplied the said drawings, specifications, or other data is not to be regarded by implication or otherwise as in any manner licensing the holder or any other person or corporation, or conveying any rights or permission to manufacture, use or sell any patented invention that may in any way be related thereto.

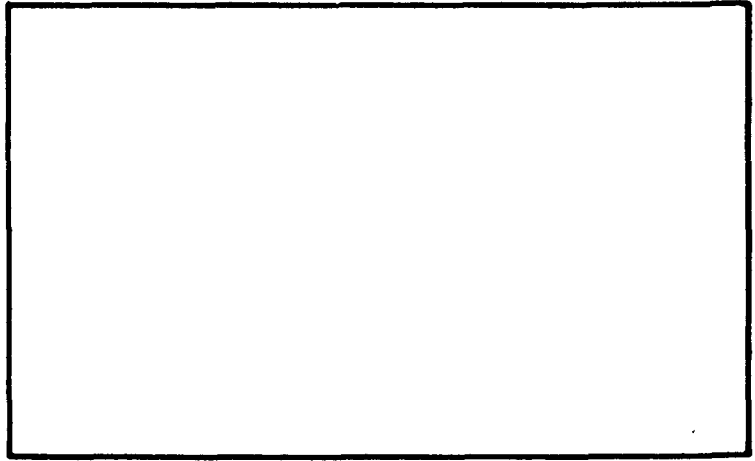
63-35

404 848

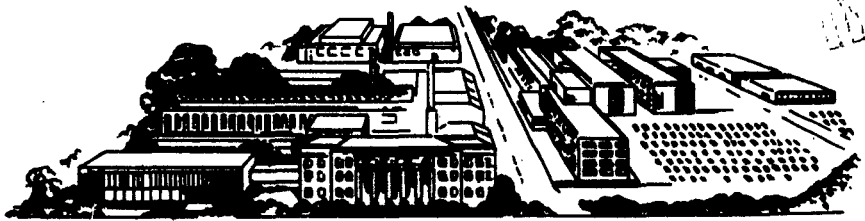
404848

RESEARCH REPORT

CATALOGED BY ASTIA
AS AD NO. _____

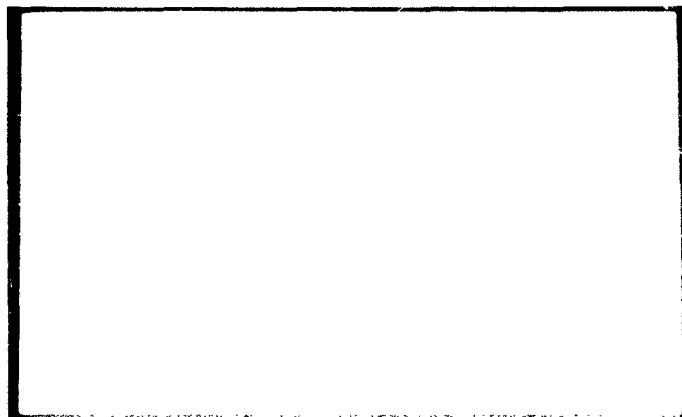


DOC
MAY 21 1963
LIBRARY OF CONGRESS



BATTELLE
MEMORIAL INSTITUTE

\$4.60



BATTELLE FIELDS OF RESEARCH

AERONAUTICAL ENGINEERING
AGRICULTURAL CHEMICALS
ALLOY DEVELOPMENT
ANALYTICAL CHEMISTRY
APPLIED MATHEMATICS
BIOCHEMISTRY
BIOPHYSICS
BUILDING AND ENGINEERING MATERIALS
CATALYSIS AND SURFACE CHEMISTRY
CERAMICS
CHEMICAL ENGINEERING
CHEMICAL PROCESSES
CORROSION TECHNOLOGY
COMPUTER ENGINEERING
ECONOMICS
ELECTRICAL ENGINEERING
ELECTROCHEMICAL ENGINEERING
ELECTROCHEMISTRY
EXTRACTIVE METALLURGY
ELECTRONICS
FERROUS METALLURGY
FOUNDRY PRACTICE
FOOD TECHNOLOGY
FUELS AND COMBUSTION
GRAPHIC ARTS TECHNOLOGY
GLASS TECHNOLOGY
HIGH-TEMPERATURE METALLURGY
HUMAN ENGINEERING
IMMUNOLOGY AND CANCER STUDIES
INDUSTRIAL PHYSICS
INFORMATION PROCESSING
INORGANIC CHEMISTRY
INSTRUMENTATION
LIGHT ALLOYS AND RARE METALS
LUBRICANT TECHNOLOGY
MECHANICAL ENGINEERING
METAL FINISHING
METALLURGICAL PROCESSES
MINERALOGY AND MICROSCOPY
MINERALS PROCESSING
MICROBIOLOGY
NONFERROUS METALLURGY
NUCLEONICS
OPERATIONS RESEARCH
ORGANIC CHEMISTRY
ORGANIC COATINGS
PETROCHEMICALS
PETROLEUM ENGINEERING
PHYSICAL CHEMISTRY
PHARMACEUTICAL CHEMISTRY
PRODUCTION ENGINEERING
PULP AND PAPER TECHNOLOGY
RADIOISOTOPES AND RADIATION
RELIABILITY ENGINEERING
REACTOR TECHNOLOGY
REFRACTORIES
RUBBER AND PLASTICS
SEMICONDUCTORS AND SOLID-STATE DEVICES
SYSTEMS ENGINEERING
TEXTILES AND FIBERS
THEORETICAL AND APPLIED MECHANICS
THERMODYNAMICS
WELDING AND METALS-JOINING TECHNOLOGY
WOOD AND FOREST PRODUCTS

ASD-TDR-62-728

DESIGN CRITERIA FOR HIGH-SPEED
POWER-TRANSMISSION SHAFTS

First Quarterly Report - Phase II

May 1963

Flight Accessories Laboratory
Directorate of Aeromechanics
Aeronautical Systems Division
Air Force Systems Command
Wright-Patterson Air Force Base, Ohio

Project No. 8128, Task No. 812802

(Prepared under Contract No. AF 33(657)-10330
by the Battelle Memorial Institute, Columbus 1, Ohio;
J. B. Day, R. G. Dubensky, H. C. Meacham, and J. E. Voorhees, authors)

Battelle Memorial Institute

5 0 5 K I N G A V E N U E C O L U M B U S I , O H I O

AREA CODE 614, TELEPHONE 299-3191

May 17, 1963

Flight Accessories Laboratory
Aeronautical Systems Division
Wright-Patterson Air Force Base
Ohio

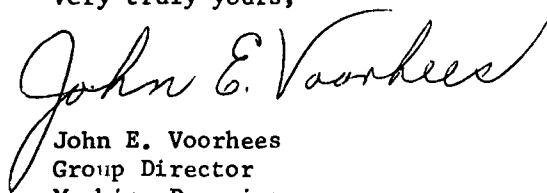
Attention ASRMFP-3
Contract No. AF 33(657)-10330

Gentlemen:

Study and Development of Design Criteria for
High-Speed Power Transmission Shafts

This is the first quarterly technical progress report to be submitted on this project, and covers the period from the start of the second phase of the project on January 15, 1963, to May 15, 1963. Fifty-three standard copies and one reproducible copy have been prepared and mailed in accordance with the distribution list of Contract AF 33(657)-10330, last revised as of the letter of May 1, 1963 (ASRDP-30).

Very truly yours,


John E. Voorhees
Group Director
Machine Dynamics

JEV: els

cc: 53 copies + 1 reproducible
According to Distribution List

DISTRIBUTION LIST

ASD (ASRPP-30, B. P. Brooks)
Wright-Patterson Air Force Base
Ohio
2 copies and 1 reproducible

Chief of Transportation
Department of the Army
ATTN: TCARD
Washington 25, D. C.
2 copies

Deputy Chief of Staff for Operations
Director, Army Aviation
Department of the Army
Washington 25, D. C.
1 copy

Commanding General
U. S. Army Transportation Material Command
P. O. Box 209, Main Office
St. Louis 66, Missouri
3 copies

Commanding Officer
U. S. Army Transportation Aviation
Field Office
ATTN: Captain Brown
Bldg. T-7, Gravelly Point
Washington 25, D. C.
1 copy

Commanding Officer
U. S. Army Transportation Research
Command Liaison Office
ATTN: MCLATS
Wright-Patterson Air Force Base, Ohio
2 copies

Commanding Officer
U. S. Army Transportation
Research Command
Fort Eustis, Virginia
7 copies

Commanding General
Continental Army Command
Fort Monroe, Virginia
(Thru WWOL-6)
1 copy

ASD (ASNDPV, Mr. Thomas)
Wright-Patterson Air Force Base
Ohio
1 copy

ASD (ASRMCS-1, Lt. Hall)
Wright-Patterson Air Force Base
Ohio
1 copy

Thompson Ramo Wooldridge, Inc.
ATTN: Elizabeth Barrett, Librarian
23555 Euclid Avenue
Cleveland 17, Ohio
1 copy

General Dynamics/Convair
ATTN: R. W. Casebolt
Mail Zone 6363
P. O. Box 1950
San Diego 12, California
1 copy

ASD (ASAPRL)
Wright-Patterson Air Force Base
Ohio
1 copy

Defense Documentation Center
Arlington Hall Station
Arlington 12, Virginia
13 copies

Technical Information Center
Aerospace Corporation
P. O. Box 95085
Los Angeles 45, California
1 copy

SSD (SSTRE, Major Iller)
AF Unit Post Office
Los Angeles 45, California
1 copy

Power Information Center
Moore School Building
200 South 33rd Street
Philadelphia 4, Pennsylvania
1 copy

DISTRIBUTION LIST

(Page -2-)

U. S. Army Mobility Command
ATTN: Mr. Lewis T. Gerbach,
AMSMO-RDT
Centerline, Michigan
1 copy

ASD(ASRMDD-23, R. Cook)
Wright-Patterson Air Force Base
Ohio
1 copy

Ray C. Ingersoll Research Center
Borg-Warner Corporation
ATTN: Mrs. Jean Summers, Librarian
Wolf and Algonquin Roads
Des Plaines, Illinois
1 copy

ASD (ASYF)
Wright-Patterson Air Force Base
Ohio
4 copies

Vertol Aircraft Corporation
Development Department, Vertol Division
ATTN: Mr. Leo Kingston
Island Road, International Airport
Philadelphia 42, Pennsylvania
1 copy

Armour Research Foundation
Illinois Institute of Technology
ATTN: R. A. Eubanks
10 West 35th Street
Chicago 16, Illinois
1 copy

Sikorsky Aircraft
511 West Monument Building
Dayton, Ohio
1 copy

The Bendix Corporation
Utica Division
ATTN: H. Troeger, Chief Engineer
Utica, New York
1 copy

Curtiss-Wright Corporation
Propeller Division
ATTN: R. H. Rue
Talbot Building
Dayton 2, Ohio
1 copy

Kaman Aircraft Corporation
ATTN: H. A. Stody
333 West First Street
Dayton 2, Ohio
1 copy

FOREWORD

The work covered by this report was accomplished under Air Force Contract AF 33(657)-10330, but this report is being published and distributed prior to Air Force review. The publication of this report, therefore, does not constitute approval by the Air Force of the findings or conclusions contained herein. It is published for the exchange and stimulation of ideas.

ABSTRACT

Standing wave ratios for 1/2-inch-diameter steel shafts, 138 inches long, were calculated for the cases in which dampers were designed to minimize vibration at the 4th and 6th critical speeds. Calculations were based on an analogy relating electrical transmission lines to high-speed shafts. The calculated standing wave ratios will be compared with measured amplitudes of vibration observed in experiments using the high-speed shaft test machine. An optical device utilizing a photocell and a light source was built to measure amplitudes of vibration along the length of the shaft. A brief study of present helicopters, taking into account engine speed, power, and helicopter size, indicated that the speed range through which power-transmission shafting will need to operate includes speeds up to the sixteenth critical speed. Shaft eccentricity measurements have been made on commercial shafts. These measurements will be used in digital computer calculations to predict actual shaft vibration amplitudes.

TABLE OF CONTENTS

	<u>Page</u>
INTRODUCTION AND SUMMARY	1
TECHNICAL WORK	3
Transmission Line Analogy Development	3
Aircraft Design Study; Damper Design; Torsional Critical Investigation	7
Design and Construction of Test Machine Changes	15
Shaft Crookedness Study	18
External Vibration Study	20
Torque Study	20
Curved Shaft Study	21
Flexible Coupling Investigation	27
Moment Absorbing Intermediate Bearing Study	27
Angular Damper Study	28
REFERENCES	30
RECORD OF RESEARCH PROGRAM	31

APPENDIX

DERIVATION OF SHAFT VIBRATION MODE NUMBER VS HORSEPOWER RELATIONSHIP	A-1
---	-----

LIST OF ILLUSTRATIONS

<u>FIGURE</u>		<u>PAGE</u>
1.	Project Progress Chart	2
2.	Rotor and Engine Speed vs Engine Horsepower	10
3.	Effect of Combining-Box Gear Ratios on Shaft Vibration Mode Number	11
4.	Effect of Diameter Ratio of Tubular Shafts of Equal Strength on Mode Number	13
5.	Shaft Vibration Mode Number vs Horsepower for Solid Shafts	14
6.	Sketch of Curved Shaft	22
7.	Modes of Vibration of Curved Shafts	24
8.	Frequency Constant for Symmetric and Anti- Symmetric Mode of Vibration vs Arc Angle for a Circular Arc	25
9.	Frequency Constant for Symmetric Mode of Vibration vs Arc Angle for a Parabolic Arc	26
10.	Diagram of Intermediate Shaft Support Bearing Which Introduces Damping by Resisting Both Lateral and Angular Motion	29

LIST OF TABLES

<u>TABLE</u>		<u>Page</u>
1.	Standing Wave Ratios For A 1/2-Inch-Diameter Steel Shaft 138 Inches Long With An Intermediate Support	6
2.	Shaft Eccentricity Measurements For 1/2-Inch-Diameter Steel Shafts, 138 Inches Long, to be Used for Experimental Verification of Transmission Line Analogy. Measurement Stations at 6-Inch Intervals	19

LIST OF SYMBOLS

C^*	=	frequency constant, dimensionless
C_a^*	=	frequency constant for anti-symmetric mode of vibration for circular arc
C_p^*	=	frequency constant for lowest frequency of vibration for a parabolic arc
C_s^*	=	frequency constant for symmetric mode of vibration for a circular arc
D	=	shaft outside diameter, inches
D_r	=	rotor diameter, inches
E	=	modulus of elasticity, pound/inch ²
I	=	section moment of inertia, inch ⁴
L	=	over-all shaft length, inches
N	=	shaft speed, rpm
N_e	=	engine speed, rpm
N_m	=	Mach number, dimensionless
N_r	=	rotor speed, rpm
P	=	shaft density, pound/inch ³
\bar{P}	=	shaft density per inch of length, pound/inch
R^*	=	radius, inches
R_g	=	gear ratio of combining box = N/N_e
R_o	=	radius measured at $\varphi = 0$, inches
S_s	=	shaft shear stress, pound/inch ²
V_s	=	speed of sound, feet/second
d	=	shaft inside diameter, inches

LIST OF SYMBOLS

(Continued)

e	=	base of natural logarithms, 2.71828...
g	=	acceleration of gravity, 386 inch/second ²
k^*	=	radius of gyration of shaft cross-section, inches
l	=	shaft length between supports, inches
l_{cs}	=	chordal length of curved shaft, inches
n	=	number of principal mode of vibration
s	=	symbol in coordinate system measuring arc length
φ	=	angle measured for line bisecting arc angle, degrees
γ	=	arc angle, degrees
ω	=	shaft critical speed, radian/second
hp_e	=	horsepower per engine
rpm	=	revolutions per minute
(VSWR)	=	voltage standing wave ratio

INTRODUCTION AND SUMMARY

The ultimate objective of this project is the establishment of a systematic design procedure for ultra-high-speed power transmission shafting. Work toward this objective involves a combination of an experimental program using reduced-scale shafts, and an analytical approach using both a digital computer program and an electrical transmission line analogy.

Figure 1 shows the progress to date on various project tasks. The open blocks indicate progress as originally planned, and the solid bars show actual progress. The number of man-hours expended during the last month is 500. The percentage of project appropriation spent to date is indicated in the last bar.

During this first quarter of Phase II, work has been concentrated on the following areas:

- (1) Analytical studies to further verify the transmission line analogy and to determine the effects of shaft curvature and mass eccentricity (crookedness) on shaft vibration.
- (2) The design and construction of modifications to the high-speed shaft test machine required to evaluate the effects on shaft dynamics of torque, shaft curvature, and externally introduced vibrations.
- (3) The design and construction of a device to measure small amplitudes of vibration along the length of the test shaft.

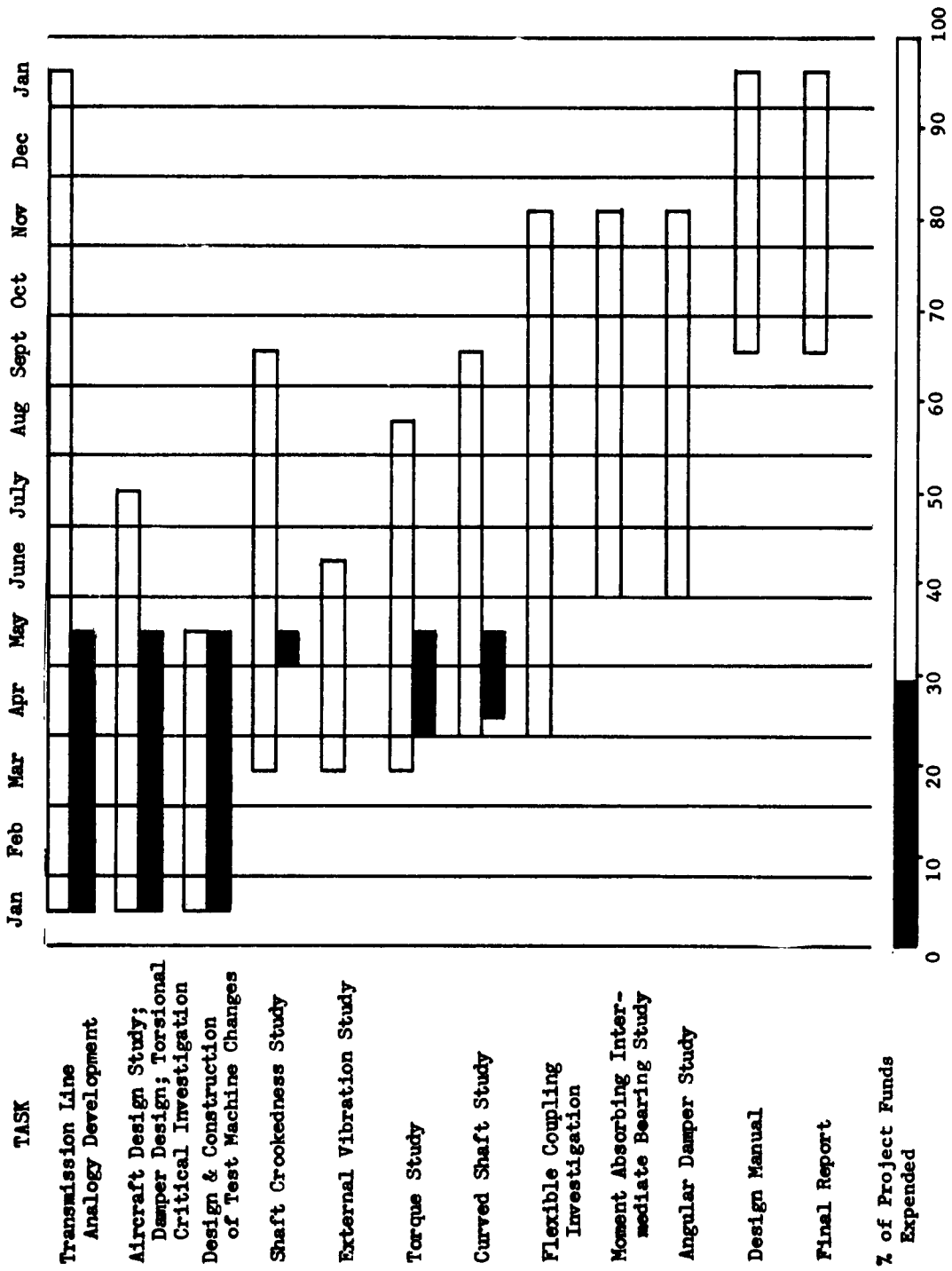


FIGURE 1. PROJECT PROGRESS CHART

- (4) A study of present helicopter design to determine the range of critical speeds through which high-speed shafting will need to operate.

TECHNICAL WORK

Note that on Figure 1, twelve research tasks are listed, the last two being the writing of the design manual and final report. This report describes briefly each of the other ten research tasks and the progress to date on each task.

1. Transmission Line Analogy Development - An analytical design procedure for high-speed power transmission shafts was developed during Phase 1 [Ref. (1)]* of this research program. This procedure was formulated using an analogy between the vibration of high-speed shafting and the voltage variation in electrical transmission lines. The electrical transmission line problem was shown to be analogous to the high-speed shaft vibration in the following manner.

Severe vibration results when the speed of rotation of a shaft corresponds to one of its natural frequencies of lateral vibration. These speeds are known as the shaft critical speeds, with the first critical speed called the first mode of vibration, the second critical the second mode, etc. The frequencies of lateral vibration and the displacements can be determined from the solution of the fourth order partial differential equation which describes the physical problem. Displacements thus obtained are a function of sinusoidal and hyperbolic terms. As the mode number

* References are given on page 30.

increases and the length-to-diameter ratio increases, the displacement curve of the shaft approaches a sinusoid, with the exception of the ends of the shaft. Thus, the displacements in the central portion of the thin shaft may be approximated by the solution of the second-order partial differential equation, or wave equation, which describes the vibration of thin shafts. However, the variation of the voltage in an electrical transmission line also is represented by a second-order partial differential equation or wave equation. Since the two systems are described by the same equations, they are said to be analogous. Thus, by using the classical electro-mechanical analogue which relates force to voltage, mass to inductance, spring constant to capacitance, and damping constant to resistance, an analogy between the high-speed power transmission shaft and an electrical transmission line may be obtained.

One of the important characteristics in electrical transmission line calculations is the voltage standing wave ratio (VSWR), as the efficiency of power transmission is directly related to the VSWR. For maximum efficiency the VSWR must be minimized, and this is done by matching the load impedance to the line impedance at the operating frequency. In Phase I of the project, expressions were developed showing that for shafts, the impedance is a function of the shaft diameter and speed, and the load impedance is a rather complex function of the damping coefficient of the bearing support, the spring rate of the bearing support, the mass of the bearing and damper, and the location of the bearing-spring-damper assembly along the shaft. Verification of the transmission line analogy involves first the calculation of the VSWR's for various shaft setups, then a measurement of amplitudes of vibration of the shaft in the high-speed

test machine, and finally a comparison of the measured amplitudes with the calculated standing wave ratios.

The shaft selected for the experimental verification of the analogy was a 1/2-inch-diameter steel shaft 138 inches long. Support spring rates, damping coefficients, and locations were determined by the design procedure developed during Phase I, whereby these parameters can be calculated after the speed at which the impedance is to be matched is chosen. Standing wave ratios were determined for the first nine critical speeds with a damper designed to give optimum operation, that is, a standing wave ratio of one, at the 6th critical speed. A second damper was designed to optimize operation at the 4th critical speed and a few standing wave ratios at other speeds were calculated for this case.

During the first quarter of this research program all calculations necessary to determine the standing wave ratios for this shaft system for all critical speeds up to the 20th were completed. These values were determined by the procedure developed in Phase I and are shown in Table 1.

As mentioned earlier, these standing wave ratios will be compared with the amplitude of vibration of the experimental shaft to verify the transmission line analogy. The measurement of the small amplitudes of vibration of the experimental shaft at all twenty critical speeds has required a great deal of investigation of measurement techniques. The measuring techniques must be accurate for high speeds, must record small amplitudes of vibration at any point along the shaft length, and must not change the shaft behavior. A vibration amplitude measuring device was

TABLE 1. STANDING WAVE RATIOS FOR A 1/2" DIA. STEEL SHAFT
138" LONG WITH AN INTERMEDIATE SUPPORT

CRITICAL SPEED MODE NUMBER	STANDING WAVE RATIO	
	SUPPORT OPTIMIZED FOR 4 th CRITICAL SPEED	SUPPORT OPTIMIZED FOR 6 th CRITICAL SPEED
1	2.95	29.
2	2.66	4.5
3	20.	1.96
4	1.0	19.
5	3.9	3.8
6	24.	1.0
7	1.77	2.4
8	6.2	8.5
9	80.	33.
10	3.35	1.73
11	14.	4.0
12	7.5	15.
13	5.6	35.
14	26.	2.45
15	5.9	6.0
16	8.3	16.0
17	31.	160.
18	4.6	2.8
19	12.	9.6
20	39.	17.

built utilizing a light source and a photo-resistive cell. The light bulb was mounted on a carriage on one side of the shaft and the photocell was positioned on the opposite side of the shaft such that the shadow of the shaft edge bisects the photocell. Photocell output voltage was viewed on an oscilloscope. This optical amplitude measuring device was calibrated by reading the output voltage for known peak-to-peak displacements.

In the first attempts to measure the amplitude of vibration of the shaft installed in the high-speed shaft test machine, it was found that the device was sensitive to position of the shadow of the shaft edge. As the carriage was moved to scan the shaft between the two intermediate supports, the sag of the shaft was sufficient to cause a 25 per cent variation in the output voltage. A gas-type phototube has been substituted for the photo-resistive cell as a readout device, and this problem has now been overcome.

This optical device will be used to determine the shaft critical speeds by monitoring the voltage and noting the speeds at which the maximum values occur. At high shaft speeds the critical speeds must be determined by this method, as the oscilloscope and all personnel remain outside the test cell.

2. Aircraft Design Study; Damper Design; Torsional

Critical Investigation - The work in this area, done in the last month, has been concerned mainly with the aircraft design study, with emphasis placed on determining the critical speed range for which high-speed shafting should be designed. In order to provide some general guideline for selecting

a critical speed range likely to be encountered in helicopter applications, a brief study of the relationship of shaft critical speed to engine power was made. Based on this limited study, it appears that the speed range most likely in practical applications, and which should be covered in the design manual, includes speeds up to the tenth critical speed. Speeds up to the sixteenth critical might occur under some conditions, so limited attention should be given to these higher vibration modes.

A summary of the design study follows. The following conditions were assumed to apply:

- (1) Only double-rotor helicopters were considered.
- (2) One engine per rotor was installed in the aircraft.
- (3) Rotor tip speed was constant at Mach 0.7.
- (4) Transmission shaft length was 60 per cent of rotor diameter.
- (5) All solutions involving changes in shaft materials or diameters were for equal-strength conditions.
- (6) The relationships between rotor rpm, engine rpm, and engine horsepower were assumed to be those shown in graphs supplied by TRECOM. The higher values of rotor rpm versus horsepower were chosen as more representative of future conditions.

A generalized equation relating shaft parameters and engine parameters was derived. The derivation is given in Appendix A. The equation was determined first for solid shafts and states the value of mode number to be:

$$n_{\text{solid}}^2 = 8.35 \times 10^8 \left[\left(\frac{P}{E} \right)^{1/2} (R_g^4 S_s)^{1/3} \right] \left[\frac{N_e^{4/3}}{(N_e - 4750)^2 \text{hp}_e^{1/3}} \right] \quad (1)$$

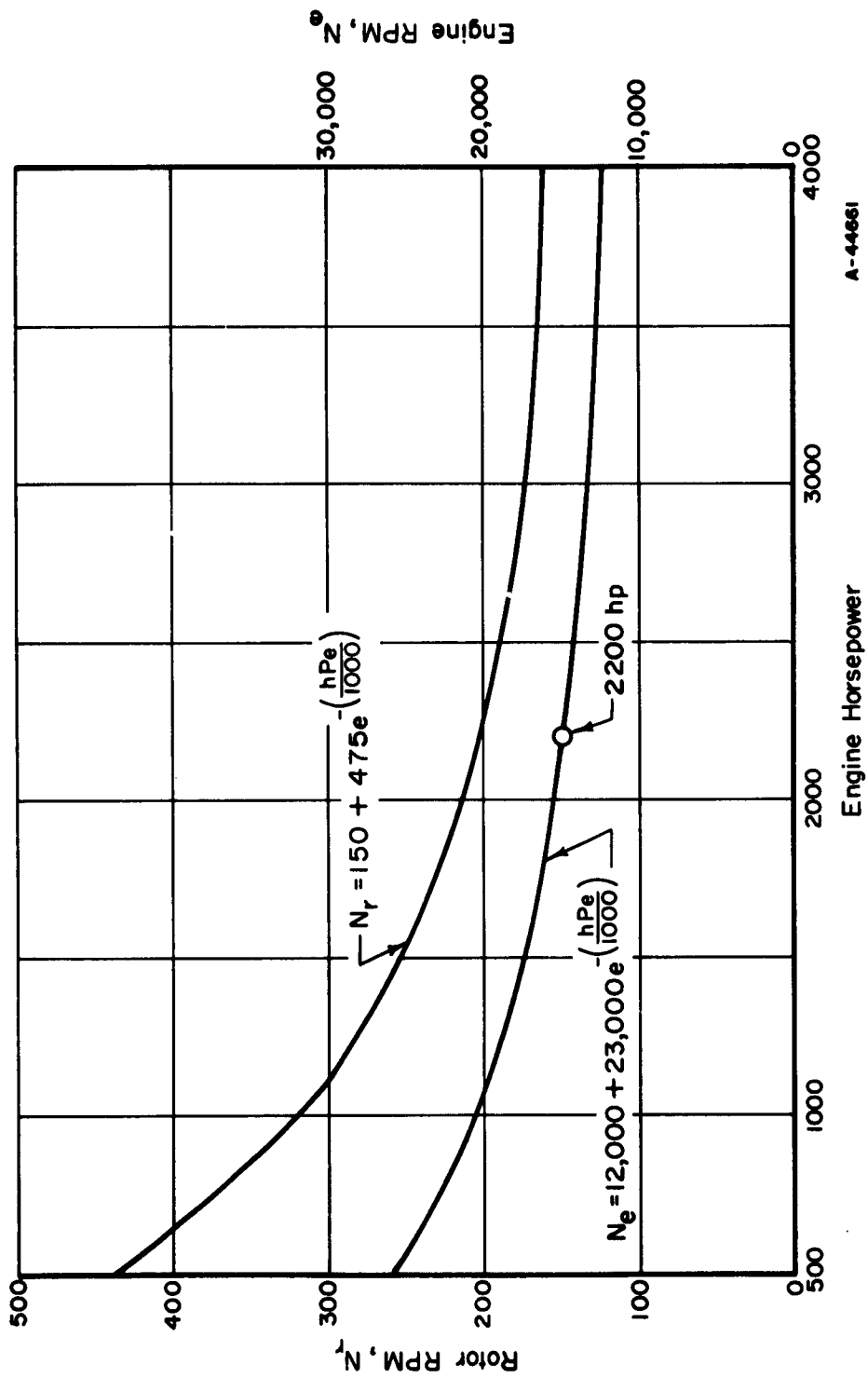
All of the items in the first bracket are design parameters, while the second bracket consists of terms which can be obtained from the plot of engine rpm vs horsepower (Figure 2) derived from the data supplied by TRECOM.

Equation (1) can be simplified for consideration of steel and aluminum shafts. Assumed values were calculated in the appendix to produce:

$$n_{\text{solid steel}}^2 = \frac{2.51 \times 10^6 R_g^{4/3} N_e^{4/3}}{(N_e - 4750)^2 (\text{hp}_e)^{1/3}} \quad (2)$$

$$n_{\text{solid aluminum}}^2 = \frac{1.61 \times 10^6 R_g^{4/3} N_e^{4/3}}{(N_e - 4750)^2 (\text{hp}_e)^{1/3}} \quad (3)$$

Two other parameters will be of general interest. Since multi-engine machines will probably have combining gear boxes, it seems likely that some speed reductions will be made in these boxes, primarily in the interest of weight reduction. From equation (1), it can be seen that the mode number n varies as the $2/3$ power of the gear ratio R_g . Figure 3 is a plot of this function. Tubular, rather than solid, shafts will probably be used in real



A-44661

FIGURE 2. ROTOR AND ENGINE SPEED VS ENGINE HORSEPOWER

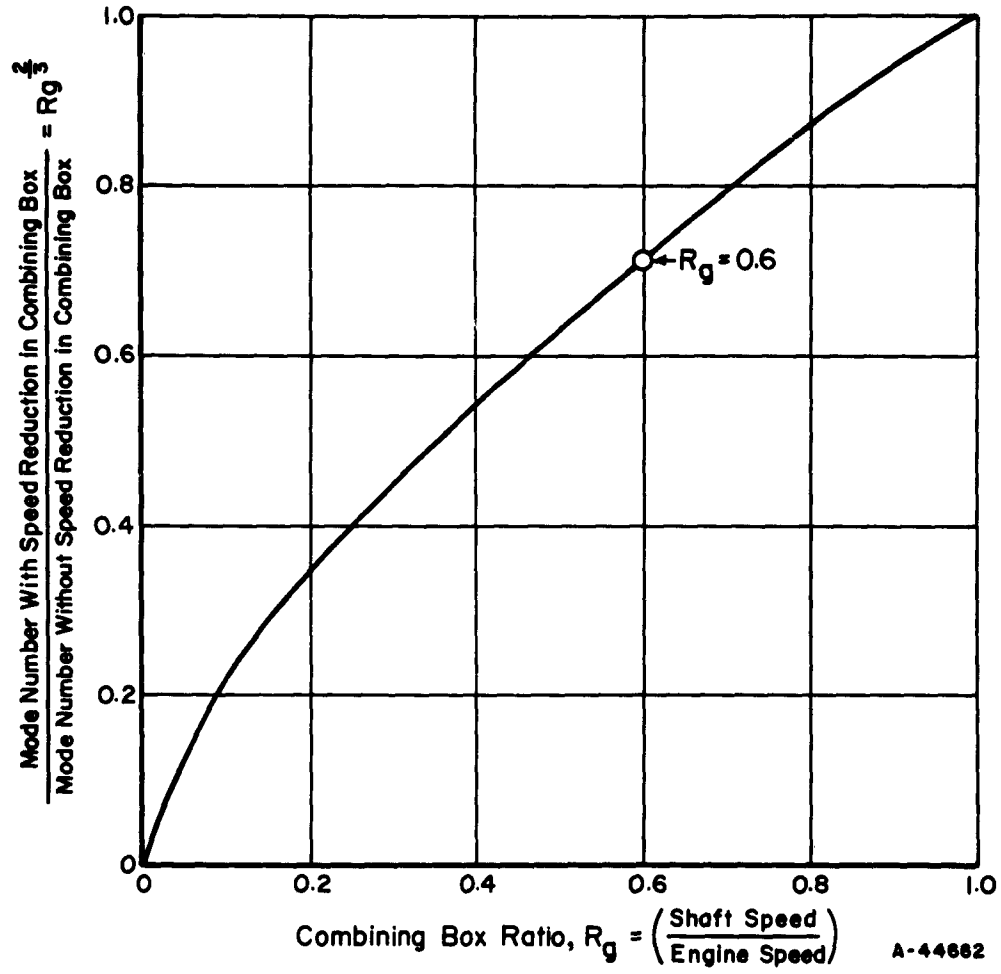


FIGURE 3. EFFECT OF COMBINING-BOX GEAR RATIO ON SHAFT VIBRATION MODE NUMBER

applications. Figure 4 shows the relationship between mode number for tubular shafts of equal strength, and their inside-to-outside diameter ratios, d/D . This figure is simply a conversion of Figure 5 of the Phase I Report.

Figure 5 presents the final relationships between mode number, shaft material, selected gear ratios, and engine horsepower. It can be seen that the mode number does not vary greatly with horsepower.

A typical example should suffice to illustrate the use of the figures. Suppose we would like to determine the probable mode number for a future application where:

Engine hp - 2200 (per engine)

Shaft - Aluminum, $d/D = 0.9$

Combining Box Gear Ratio = $R_g = 0.6$

From Figure 2, $N_e = 14,800$ rpm

For a solid aluminum shaft, with $R_g = 1.0$, we find the probable mode number from Figure 5 to be 18.7.

The mode number for $R_g = 0.6$ can be determined by multiplying the factor from Figure 3 by the mode number for $R_g = 1$, giving a "geared down" mode number for a solid shaft of 0.71×18.7 , or 13.28.

One final step remains - the conversion of the mode number for a solid shaft into that of a tubular shaft whose inside diameter is 0.9 times its outside diameter. Figure 4 provides a conversion factor of 0.72, which when multiplied by 13.28 gives the final answer. The mode number is 9.56, meaning that a shaft with simply-supported ends would operate just above its ninth critical speed in this application.

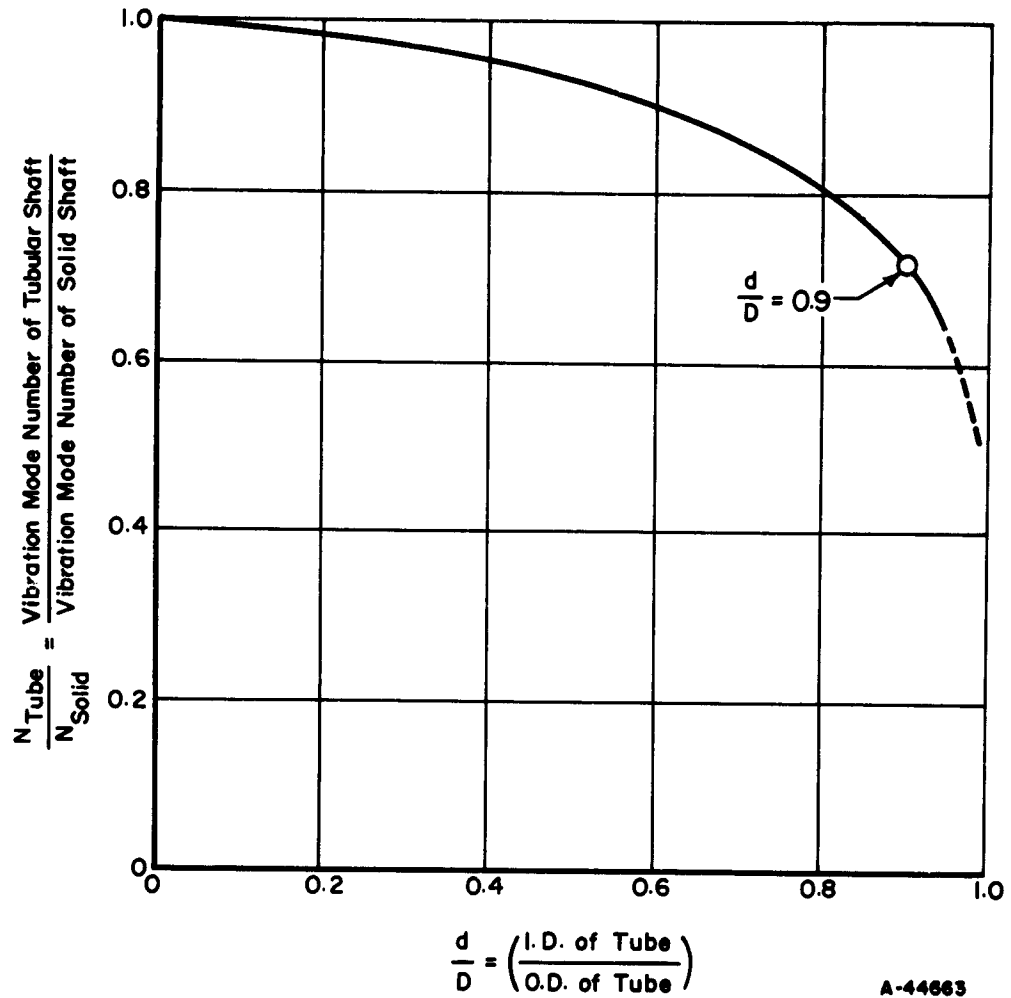


FIGURE 4. EFFECT OF DIAMETER RATIO OF TUBULAR SHAFTS OF EQUAL STRENGTH ON MODE NUMBER

A-44663

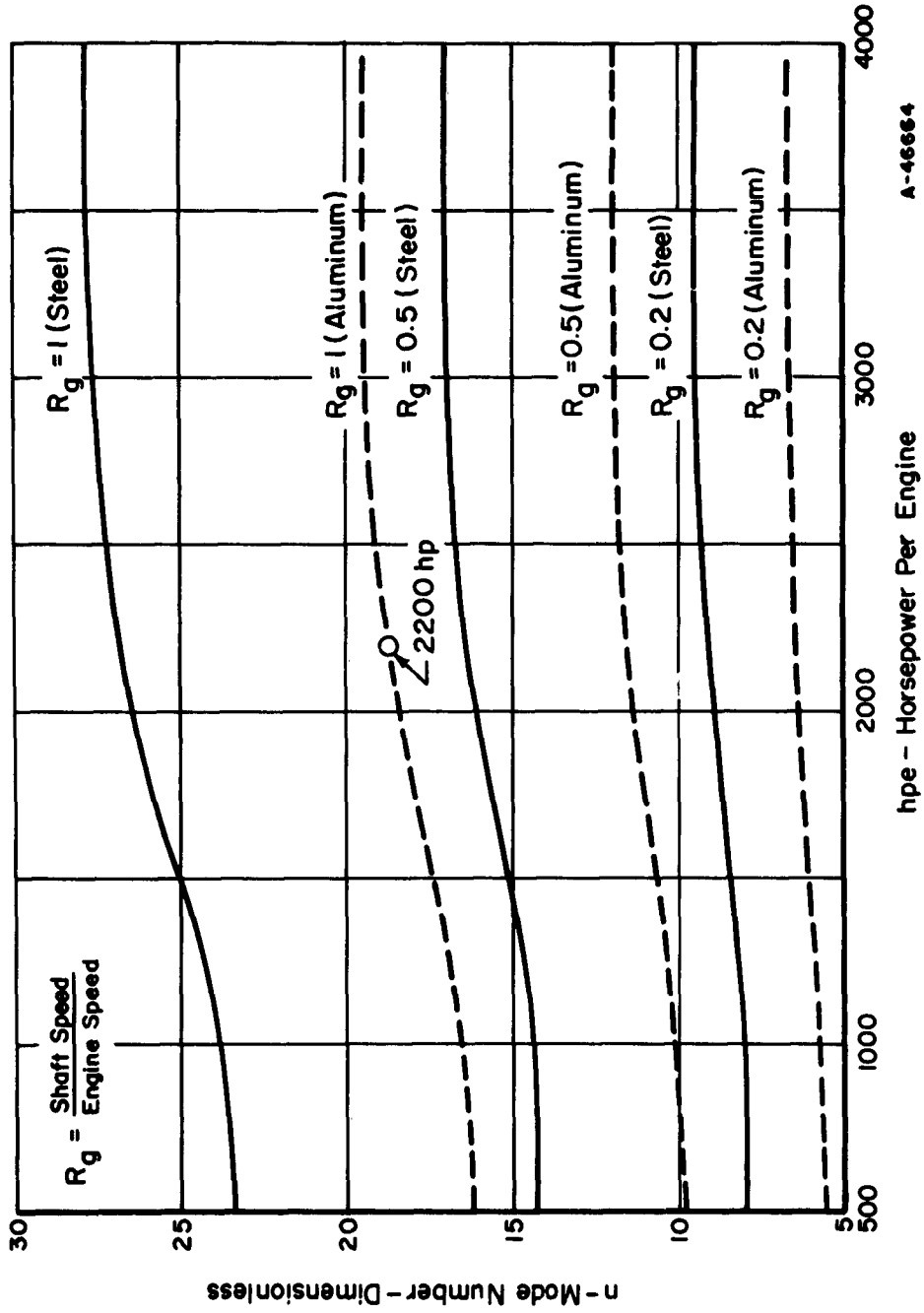


FIGURE 5. SHAFT VIBRATION MODE NUMBER VS HORSEPOWER TRANSMITTED THROUGH SOLID SHAFTS

It might be worthwhile to attempt some generalizations on the results obtained. Tubular shafts will almost certainly be used, and a diameter ratio (d/D) of 0.9 is conservative. (The Chinook shaft, for example has a ratio of 0.948. Aluminum is a likely shaft material. Most combining boxes will probably have some reduction built in, and a 2:1 reduction ($R_g = 0.5$) would seem to be a reasonable value. From these assumptions and Figures 4 and 5, we could determine the highest probable mode number to be $11.6 \times 0.72 = 8.35$, just above the eighth critical speed. Allowing some margin for error, we might conclude that the research effort should be concentrated on speeds up to the tenth critical, with limited attention being given to speeds up to the sixteenth critical ($R_g = 1$, $d/D = 0.8$).

3. Design and Construction of Machine Modifications - A

considerable portion of the first quarter's work on this project has been concentrated on the design and construction of the modifications for the high-speed shaft test machine which are required to evaluate the effects of torque, shaft curvature and vibration, and to measure small amplitudes of shaft vibration.

The setup to be used for making tests of a torqued shaft has been discussed in the monthly letter reports. In summary, it was originally planned to apply torque to the shaft by driving it at one end and braking it at the other end by means of an eddy-current brake or a prony brake. This idea was discarded in favor of a system utilizing a second shaft parallel with, and geared to, the test shaft. Torque in such a system is proportional to the shaft windup which is originally applied. This

system was preferred because it eliminated construction of a prony brake and requires only enough additional power from the drive system to overcome the induced friction torque.

During the last month, components for this system were completed and the system was demonstrated on April 29 in the presence of Mr. Wayne Hudgins and Mr. Donald Kane of TRECOM. It was found that axial forces were developed in the test shaft with this setup. Although the gears are spur gears and should not introduce axial forces, the flexing of the shaft during operation evidently moves the end of the shaft, developing a force which is held in by the gear tooth face friction. The gears are, of course, under load due to the torque in the system.

Previous analytical and experimental work in Phase I showed that shaft operation is quite sensitive to axial force, therefore axial forces must be minimized if the effects of torque are to be determined. Accordingly, camrollers will be placed on the brake end support of the torqued shaft to ensure that significant axial forces cannot be developed. Drawings for the modified assembly have been completed and it is hoped that all modifications will be completed by the end of May.

In preparation for the curved-shaft tests, an additional bed for the high-speed shaft test machine was designed and built. This bed allows the brake end of the shaft to be displaced up to 24 inches laterally with respect to the drive end. By proper adjustment of the brake end, varied curves can be obtained in the shaft, ranging from an S-curve in which both ends of the shaft are parallel but displaced laterally, to an arc of a circle.

Additional modifications are required to allow torque to be applied to the curved shaft. The ends of the torque "return" shaft will also be displaced by the same amount as the test shaft; it is probable that two or more universal joints will be used in this shaft to accommodate its misalignment. Changes will be made at the brake end to allow it to float axially in the same manner as the straight shaft.

Other machine modifications completed include the carriage-mounted optical pickup. This unit, described in a previous section, is now being calibrated. In general, the majority of basic machine modifications have been completed, although detail changes may be required continually during the experimental portions of the project.

4. Shaft Crookedness Study - In the past month, measurements of mass eccentricity, or shaft crookedness, along the shaft were made. Two steel shafts, 1/2-inch-diameter and 138 inches long, were measured with the shafts installed in the test machine. This measurement was completed with an optical telescope mounted on a vertical micrometer scale. Two measurements were made in the plane of maximum eccentricity, and a subtraction of the values gave the deviation of the shaft from a straight line. Table 2 shows the values of these shaft eccentricity measurements. These values are an indication of the straightness of the experimental shafts and will be used in the computer program to predict vibration amplitudes.

Computer work has been conducted with the objective of correlating calculated amplitudes of vibration with the experimental amplitudes of vibration and with the standing wave ratios, taking into account the effect of mass eccentricity. Two computer programs must be used to calculate the amplitudes of vibration. The first, a shaft critical-speed program, is used to calculate the particular critical speed. This speed is then substituted into the second computer program, the shaft-deflection program, which calculates the amplitude of vibration. The measured shaft eccentricities were included in these computer programs, with the objective of calculating the amplitude of vibration for the ninth critical speed of the experimental shaft used with a support optimized for the sixth critical speed. However, in all attempts to calculate this critical speed, the computer has stopppd calculating after the second input speed. The computer program will be examined for possible causes of improper results.

TABLE 2. SHAFT ECCENTRICITY MEASUREMENTS FOR 1/2-INCH-DIAMETER STEEL SHAFTS, 138 INCHES LONG, TO BE USED FOR EXPERIMENTAL VERIFICATION OF TRANSMISSION LINE ANALOGY. MEASUREMENT STATIONS AT 6-INCH INTERVALS.

Station No.	Mass Eccentricity - Inches	
	Shaft No. 1	Shaft No. 2
1	-.000985	-.00197
2	.000	.000
3	.000	-.00394
4	-.000985	-.0059
5	+.00197	-.0059
6	+.00492	-.00788
7	+.0128	-.00688
8	+.0177	-.00688
9	+.0187	-.00492
10	+.0197	-.00196
11	+.0177	-.00196
12	+.014	.000
13	+.00886	-.00196
14	+.0128	-.00196
15	+.0118	-.00196
16	+.014	-.00196
17	+.01475	-.000985
18	+.0128	.000
19	+.0108	+.00295
20	+.00985	+.00295
21	+.0059	+.001965
22	+.00394	.000
23	+.00197	-.00295
24	-.00197	.000

Upon resumption of computer calculations, the critical speeds will be calculated for the shaft configuration with support characteristics optimized for the fourth and sixth critical speeds. The amplitudes of vibration will be calculated using the measured mass eccentricities. Experimental measurements of amplitudes of vibration of the two specific shafts will be made and correlated with calculated values. Both of these will in turn be correlated with the previously calculated standing wave ratios.

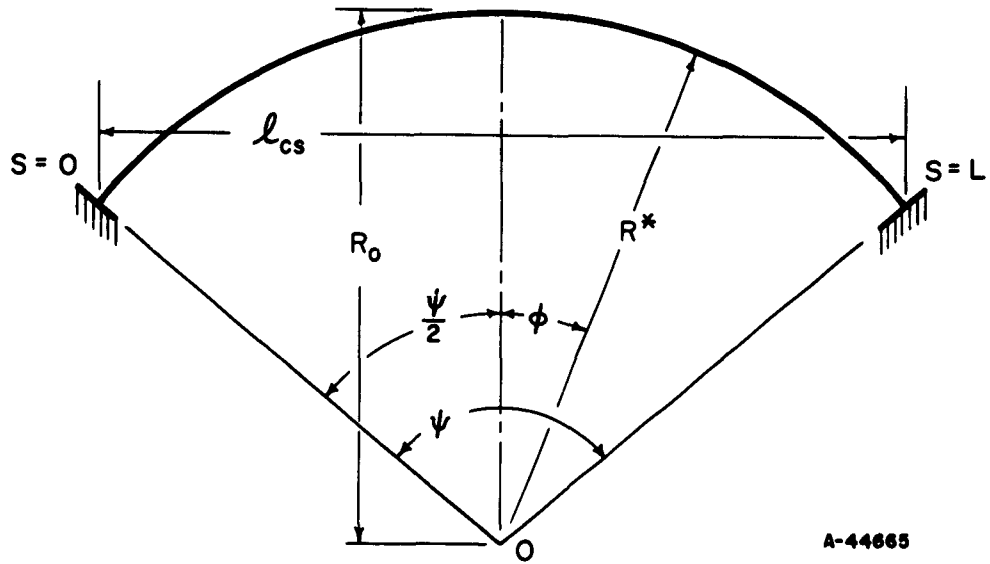
5. External Vibration Study - This study will be made to determine the effect, if any, of external vibrations on the shaft vibration characteristics. An attempt will be made to introduce to the experimental shaft setup vibrations similar to those found in present flight vehicles. Information has been received to the effect that the vibrations which occur in helicopters have predominant frequencies in the range of 4 to 30 cps. Therefore, vibrations of this frequency will be introduced into the laboratory test setup by means of a "shaker". Details for this system have not yet been decided, but should be completed by July 1, 1963.

6. Torque Study - Experimental runs giving good data on torqued-shafts have not yet been made, due to the fact that additional modifications to the experimental setup are required. However, runs using torqued shafts will be made as soon as the modifications to the high-speed shaft test machine are completed, which should be during May, 1963.

7. Curved Shaft Study - The problem of determining the shaft critical speed for curved shafts is important to the development of the design criteria for power transmission shafts, as elastic deflections of the flight vehicle introduce curvature to the drive shaft. Shaft curvature was investigated analytically during the first quarter of the research program.

A search of the technical literature shows that the problem of calculating the frequency of lateral vibration of an arc has been solved by approximate methods. It should be recalled that the critical speed corresponds to the frequency of lateral vibration. The exact solution of the problem is extremely complicated and to date only values for the lowest natural frequencies are available. Results pertaining to curved power transmission shafts are discussed for a shaft curved in the form of an arc and restrained with fixed ends. All results are for vibrations occurring in the plane of initial curvature of the arc. Figure 6 shows the shaft curved in arc, and defines the properties of the shaft.

The fundamental frequency of in-plane vibration has been determined for circular, cycloidal, catenary, and parabolic arcs. (References 2, 3, and 4). Of these curves, the circular and parabolic arcs have the greatest interest for this study. The frequency equation is given for all forms of arcs, but this discussion will be restricted to curves of circular and parabolic arcs. For detailed information on the other arc forms Reference 4 should be consulted.



A-44665

FIGURE 6. SKETCH OF CURVED SHAFT

The fundamental mode of in-plane vibration for a circular arc exhibits a crossover from a symmetric mode shape to an anti-symmetric mode shape of vibration as the arc angle ψ is increased from small values. These forms of vibration are illustrated in Figure 7a and Figure 7b. The symmetric mode shape corresponds to the lowest natural frequency mode shape for the straight shaft, and the anti-symmetric mode shape corresponds to the second harmonic mode shape for the straight shaft. The frequency of vibration for the symmetric and anti-symmetric modes of vibration is given by Equation 4.

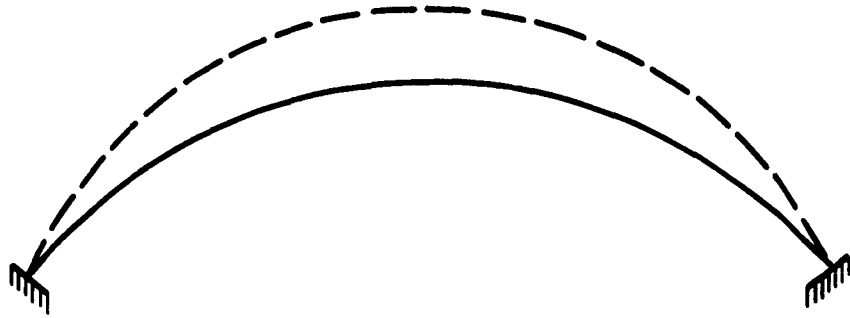
$$\omega = C^* \frac{1}{(\ell_{CS})^2} \left(\frac{EIg}{P} \right)^{1/2} \quad (4)$$

The value of the frequency constant C^* depends upon the type of vibration. For a symmetric mode of vibration, the constant is a function of the radius of curvature, the radius of gyration of the shaft, and the arc angle. Equation 5 gives the value of the constant C_s .

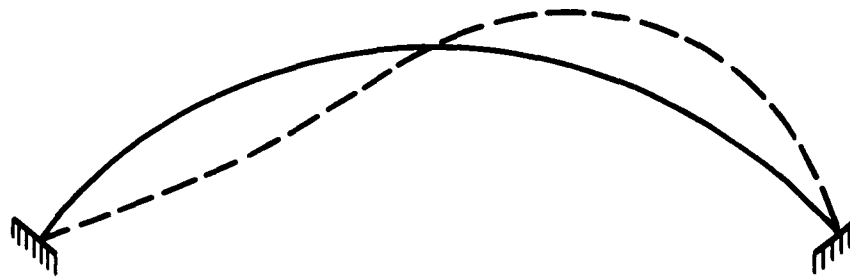
$$C_s = 4 \sin^2 \frac{\psi}{2} \left(\frac{2}{3} \frac{R_o}{k^*} + \frac{1}{3} \left(\frac{4\pi^2}{\psi} - 1 \right)^2 \right)^{1/2} \quad (5)$$

For the anti-symmetric mode of vibration, the constant is a function of the arc angle ψ , and is shown in Figure 8. This figure also shows values of C_s for various ratios of R_o/k^* . Figure 8 shows that the fundamental mode of vibration will cross over from a symmetric mode shape to an anti-symmetric mode shape in the range of small arc angles.

Equation 4 may be used to calculate the fundamental frequency of vibration for a parabolic arc if the constant C^* is placed by the constant C_p . Values of C_p as a function of the arc angle ψ for various values of R_o/k^* are shown in Figure 9.



a. Symmetric or Extensional Mode of Vibration



b. Anti-Symmetric or Inextensional Mode of Vibration

A-44866

FIGURE 7. MODES OF VIBRATION OF CURVED SHAFTS

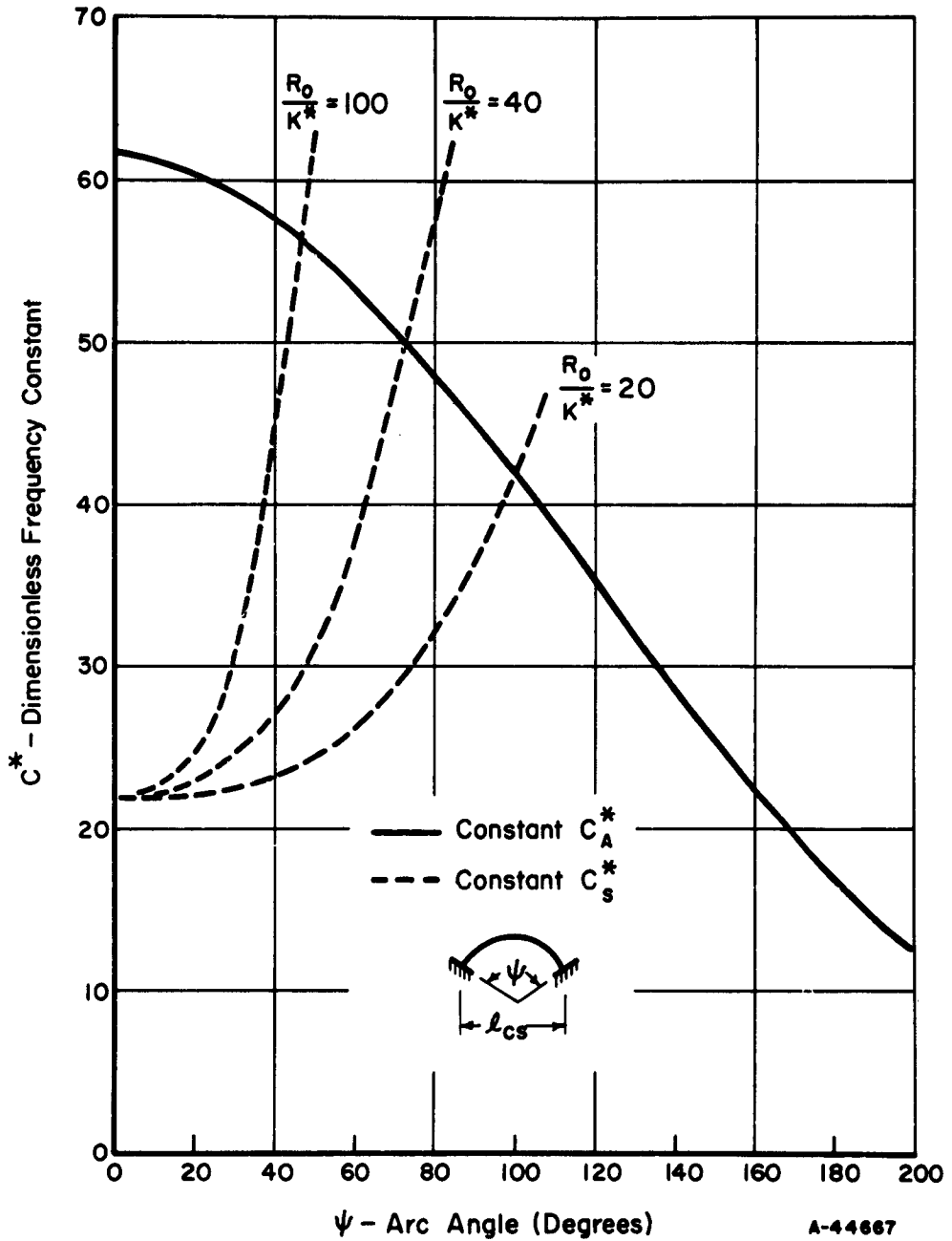


FIGURE 8. FREQUENCY CONSTANT FOR SYMMETRIC AND ANTI-SYMMETRIC MODE OF VIBRATION VERSUS ARC ANGLE FOR A CIRCULAR ARC

A-44667

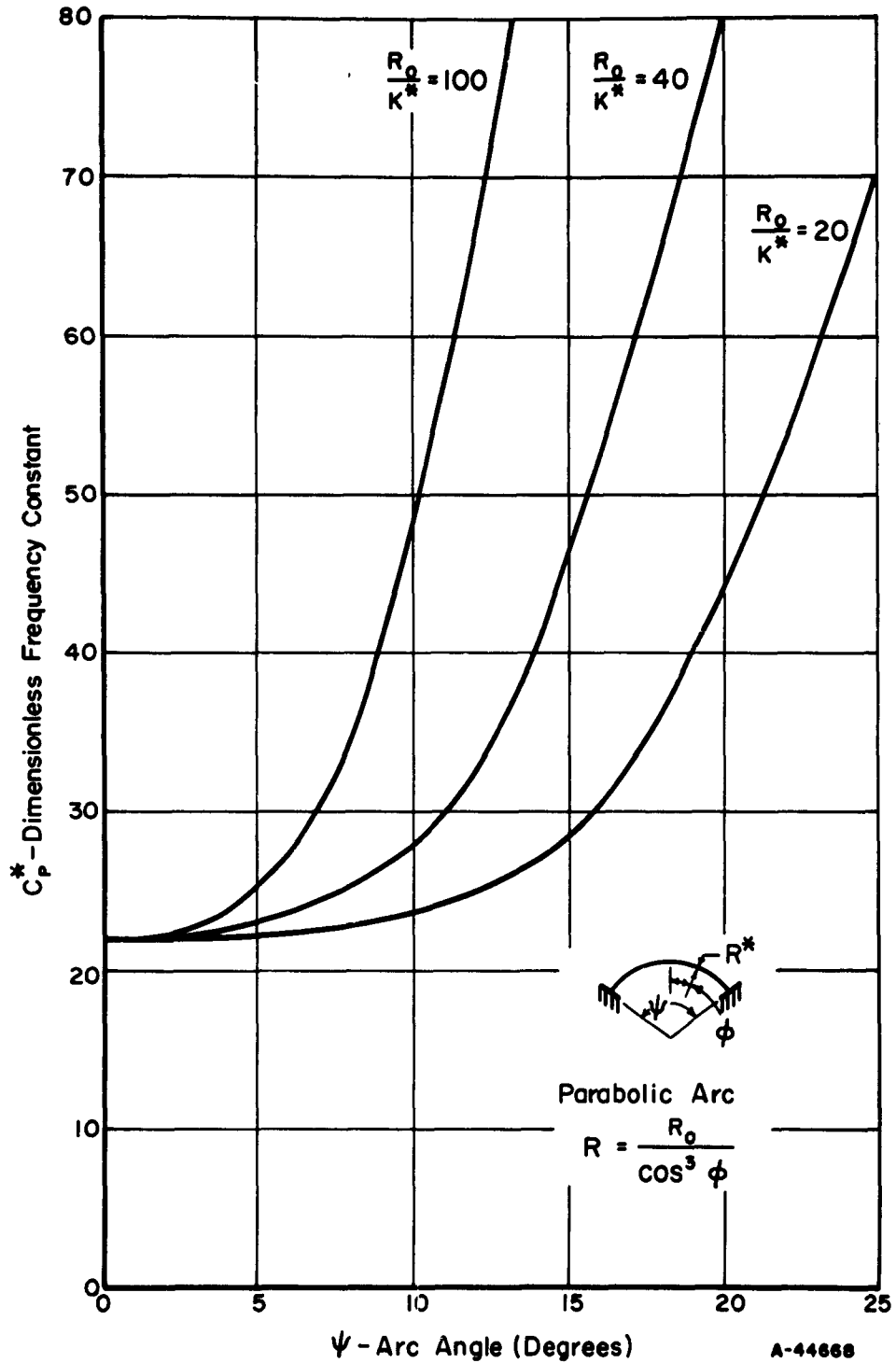


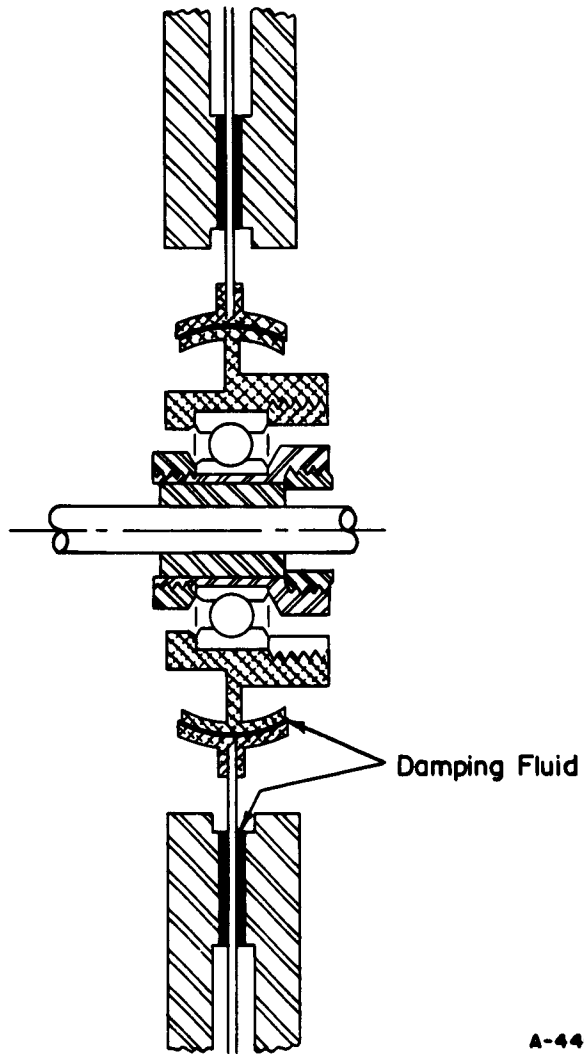
FIGURE 9. FREQUENCY CONSTANT FOR SYMMETRIC MODE OF VIBRATION VERSUS ARC ANGLE FOR A PARABOLIC ARC

A-44668

8. Flexible Coupling Investigation - The purpose of this investigation is to determine the effect of flexible couplings such as are commonly used in long shaft systems. As agreed verbally, the effects of a flexible coupling will be simulated by turning down a short length of the shaft to a smaller diameter. For example, using a 1/2-inch diameter steel shaft, an area at each end of the shaft close to the gripping collets will be reduced to a diameter of 1/4 inch for a length of one inch for one series of tests, and to 1/8 inch for another series of runs. These same diameters will also be used with tubular shafts; it will be necessary to machine a plug which can be welded or otherwise attached to the tubular shaft. The necked-down diameter introduces a low bending rigidity, as does a flexible coupling. In order to simulate and evaluate coupling mass on the necked-down shaft tests, collars will be attached to the shaft adjacent to the necked-down sections.

9. Moment - Absorbing Intermediate Bearing Study - Work on this item is not scheduled to begin until June. Work planned is the replacement of the flexure plate presently used in an intermediate support by a more rigid plate. A damper using a rigid plate will allow lateral motion of the shaft but will restrict angular motion of the shaft at the damper. The effects of this type of damper on shaft vibration characteristics will then be evaluated.

10. Angular Damper Study - Final design of this damper type has not yet begun, but the configuration to be used is shown in Figure 10. In this unit, damping would be produced by shearing the oil film between the ball and socket as the ball oscillates in the plane of the shaft. Therefore a damping action would be obtained even if the damper were located at a node position on a vibrating shaft. The construction of this damper should be well under way by the middle of June.



A-44669

FIGURE 10. DIAGRAM OF INTERMEDIATE SHAFT SUPPORT BEARING WHICH INTRODUCES DAMPING BY RESISTING BOTH LATERAL AND ANGULAR MOTION

REFERENCES

- (1) Dubensky, R. G., Mellor, Jr., C. C., Voorhees, J. E., "Design Criteria For High-Speed Power-Transmission Shafts, Part 1. Analysis Of Critical Speed Effects And Damper Support Location". Aeronautical Systems Division Technical Report, ASD-TDR-62-728, August, 1962.
- (2) den Hartog, J. P., "The Lowest Natural Frequency Of Circular Arcs", *Philosophical Magazine*, Vol. 5, Series 7, No. 28, Fe. 1928, p. 400.
- (3) Nelson, F. G., "In-Plane Vibration Of A Simply Supported Circular Ring Segment", *Int. J. Mech. Sci.*, Vol. 4, 1962, pp 517-527.
- (4) Volterra, E. and Morell, J. D., "A Note On The Lowest Natural Frequency Of Elastic Arcs", *Journal of Applied Mechanics*, *Trans. ASME*, December, 1960, p. 744.

RECORD OF RESEARCH PROGRAM

Data upon which this report is based may be found in
Battelle Laboratory Record Books, Numbers: 19932 and 19933.

APPENDIX

DERIVATION OF SHAFT VIBRATION MODE NUMBER
VS HORSEPOWER RELATIONSHIP

APPENDIX A

DERIVATION OF SHAFT VIBRATION MODE NUMBER
VS HORSEPOWER RELATIONSHIP

Two graphs relating engine and rotor rpm to horsepower were furnished by TRECOM. Curves were fitted to these graphs and equations were determined. Figure 2, page 10, shows the plot of the equations.

In order to provide a reasonable basis for calculations, the following assumptions are made:

- (1) Double-rotor helicopters are considered.
- (2) There is one engine for each rotor.
- (3) Rotor tip speed is Mach 0.7.
- (4) Shaft length equals 60 per cent of rotor diameter.

The entire set of relations will be derived for solid shafts, and then modified for tubular shafts.

Calculations

The equations derived for the curves of the two graphs supplied by TRECOM are:

$$N_e = 12,000 + 23,000 e^{-(hp_e)/1000} \quad (1)$$

$$N_r = 150 + 475 e^{-(hp_e)/1000} \quad (2)$$

These curves are considered to be valid in the range from 500 hp to 4,000 hp.

The Phase I report (Equation 3) defines the horsepower that can be carried by a solid shaft as:

$$hp = 3.12 \times 10^{-6} S_g ND^3 \quad (3)$$

Equations (5) and (7) of the first phase report define critical speeds or mode numbers in terms of rpm as:

$$N = \frac{467 D n^2}{l^2} \frac{E}{F}^{1/2} \quad (4)$$

From the definition of the limitation of rotor tip speed, we can write:

$$D_r = \left(\frac{12}{N_r} \right) \frac{60V_s N_m}{\pi}, \text{ or, since} \quad (5)$$

$$V_s = 1100 \text{ fps,}$$

$$N_m = 0.7.$$

$$D_r = \frac{176,400}{N_r} \quad (6)$$

We can write our final assumption as:

$$L = 0.6D_r \quad (7)$$

All further calculations will simply be manipulations of equations (1) through (7).

Rewriting (1) and (2):

$$e^{-(hp_e)/1000} = \frac{N_r - 150}{475} \quad (8)$$

$$e^{-(hp_e)/1000} = \frac{N_e - 12,000}{23,000} \quad (9)$$

Combining (8) and (9) yields

$$N_r = \frac{N_e - 4,750}{48.5} \quad (10)$$

Rewriting (6) as

$$N_r D_r = 176,400 \quad (11)$$

and combining with (7) yields

$$N_r L = 106,000 \quad (12)$$

Rewriting (12) and combining with (10) gives

$$\frac{N_e - 4,750}{48.5} = \frac{106,000}{L} \quad (13)$$

Or, in terms of L,

$$L = \frac{5.16 \times 10^6}{N_e - 4,750} \quad (14)$$

For convenience in solving for mode number, (4) can be rewritten as:

$$n^2 = \frac{N L^2}{467D} \left(\frac{P}{E} \right)^{1/2} \quad (15)$$

Substituting equations (3) and (14) in (15) gives:

$$n^2 = \left(\frac{P}{E} \right)^{1/2} \left(\frac{N}{467} \right) \left(\frac{5.16 \times 10^6}{N_e - 4,750} \right)^2 \left(\frac{3.12 \times 10^{-6} S_s N}{(hp_e)} \right)^{1/3} \quad (16)$$

Since for multi-engine applications a combining box will be present, it will generally be convenient to take some speed reduction in this box. Defining

$$N = R_g N_e \quad (17)$$

and simplifying (16) yields

$$n^2 = 8.35 \times 10^8 \left[\left(\frac{P}{E} \right)^{1/2} \left(R_g^4 S_s \right)^{1/3} \right] \left[\frac{N_e^{4/3}}{(N_e - 4750)^2 (hp_e)^{1/3}} \right] \quad (18)$$

The terms appearing in the first bracket are potential variables in the system, and the terms in the second bracket can be read from the graphs supplied by TRECOM. Equation (18) is a general solution for a solid shaft. For the present time, we will consider only two materials, steel and aluminum. The constants for these materials will be assumed to be:

$$\text{Steel: } S_s = 30,000 \text{ psi, } \left(\frac{P}{E}\right)^{1/2} = 9.66 \times 10^{-5}$$

$$\text{Aluminum: } S_s = 8,000 \text{ psi, } \left(\frac{P}{E}\right)^{1/2} = 9.66 \times 10^{-5}$$

Since $\frac{P}{E}$ is the same for both materials, at any set of conditions, we can calculate the value of n for a steel shaft and determine n for the aluminum shaft from

$$\frac{n_{\text{steel}}^2}{n_{\text{aluminum}}^2} = \left(\frac{S_s \text{ steel}}{S_s \text{ aluminum}}\right)^{1/3} \quad (19)$$

or,

$$\frac{n_{\text{steel}}}{n_{\text{aluminum}}} = \left(\frac{30,000}{8,000}\right)^{1/6} = 1.246, \text{ or} \quad (20)$$

$$n_{\text{aluminum}} = 0.803 n_{\text{steel}} \quad (21)$$

Substituting values in (18) gives, for solid steel shafts,

$$n_{\text{steel}}^2 = \frac{2.51 \times 10^6 R_g^{4/3} N_e^{4/3}}{(N_e - 4750)^2 (hp_e)^{1/3}} \quad (22)$$

for solid aluminum shafts:

$$n_{\text{aluminum}}^2 = \frac{1.61 \times 10^6 R_g^{4/3} N_e^{4/3}}{(N_e - 4750)^2 (hp_e)^{1/3}} \quad (23)$$